tures with spherical-like morphology, is however difficult to generate because the polydimethylsiloxane nanospheres are encapsulated in the polystyrene matrix (**Fig. 1(c)**).

For further investigation of the effect of homopolymer (polystyrene) on the microphase-separated morphologies of one-dimensional block copolymer/homopolymer nanostructures, various molecular weights of homopolymer were applied. In this way, the compatibility between block copolymer and homopolymer could be tuned. Here, homopolymers with three different molecular weights (4.7, 24, and 820 kg/mol of polystyrene, which are referred to as $hPS_{4.7k}$, hPS_{24k}, and hPS_{820k}, respectively) are applied to the polymer blends. Transition electron microscopy was used to characterize the morphology of the block copolymer/homopolymer nanostructures and corresponding diagrams are constructed (**Fig. 2**). As the molecular weight of homopolymer increases, the compatibility and miscibility between the homopolymer and block copolymer decreases, leading to the domination of macrophase-separation over microphase-separation, which would not generate morphology transitions. For the block copolymer/small-molecular-weight homopolymer (hPS_{24k}) nanostructures, multihelical morphology and spherical morphology with higher ordering of polydimethylsiloxane spheres can be observed. While for the block copolymer/high-molecular-weight homopolymer (hPS_{820k}) nanostructures, only concentric lamellar morphologies can be obtained, and a macrodomain of high-molecular-weight homopolymer (hPS_{820k}) is also observed, as indicated by the red arrow in **Fig 2**.

This work demonstrates the control of microphase-separated morphologies of block copolymer/homopolymer nanostructures by tuning the blending ratios and the molecular weights of homopolymer. In addition, three special morphologies (concentric lamellar morphology, multihelical morphology, and spherical-like morphology) can be obtained. These unique one-dimensional nanostructures mighty be further utilized by refilling with functional metals or organic dyes for the applications of sensing and drug delivery. (Reported by Jiun-Tai Chen, National Chiao Tung University)

This report features the work of Ming-Hsiang Cheng, Jiun-Tai Chen and their co-workers published in ACS Appl. Mater. Interfaces ***9****, 21010 (2017)*

TLS 23A1 IASW – Small/Wide Angle X-ray Scattering

- SAXS
- Polymer Science, One-dimensional (1D) Nanostructures, Soft Matter

References

1. M. H. Cheng, Y. C. Hsu, C. W. Chang, H. W. Ko, P. Y. Chung, and J. T. Chen, ACS Appl. Mater. Interfaces **9**, 21010 (2017).
2. C. J. Chu, P. Y. Chung, M. H. Chi, Y. H. Kao, and J. T. Chen, Macromol. Rapid Commun. **35**, 1598 (2014).
3. M. H. Cheng, H. W. Ko, P. Y. Chung, C. W. Chang, and J. T. Chen, Soft Mater. **12**, 8087 (2016).

"I WILL BE BACK! – THE RETURN OF RUBBER:" A New Mechanism to Overcome the Dilemma of Shape Fixing and Recovery in Biodegradable Polyurethane Elastomer

Structural characteristics of shape-memory polyurethane elastomer dominate the shape-memory effect while retaining the elasticity.

This is a story about the come back of rubber.

Rubber, more formally known as an elastomer, is a category of materials that respond to a force with instantaneous or temporary deformation. This feature indicates also that an elastomer is quite absent-minded, *i.e.* it

generally does not remember its previous shape. Expressed alternatively, because elastomers do not memorize a shape, they can alter their shape freely according to the instructing force applied to them. According to this point of view, elastomers are philosophically in contrast to shape-memory materials. This concept is explained in **Fig. 1**.

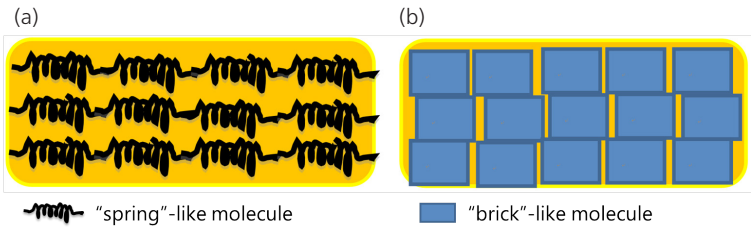

Fig. 1: (a) Rubber is composed of many spring-like molecules. (b) The shape-memory materials require a brick-like crystalline domain to fix the shape. [Reproduced from Ref. 1]

Making rubber remember is not, however, entirely impossible. Shape memory is a valuable characteristic, especially of materials used in medicine. Imagine having a small device enter the body as a result of minimally invasive surgery and then having the device expand *in situ* to repair a defective body part! It is thus highly valuable to have a shape-memory elastomer that is also biodegradable so that no secondary surgery is required to remove it from the body!

One key to develop such a biodegradable elastomer is to use the polymer polyurethane, which is a broad-category polymeric rubber material. A polyurethane molecule has soft domains that contribute to elasticity; we can make this part biodegradable. The remaining challenge is to give it memory. How can we make polyurethane resume the predesigned shape and, at the same time, let it remain free to alter shape as rubber?

The key point is the switch. When the switch is off, it is elastic with a shape-changing possibility; when the switch is on, it reverts to the shape that is preinstalled. To identify the critical reason for the rubber to memorize, we prepared three distinct materials: one is polyurethane with pure polycaprolactone diol (PCL diol) in the soft domains; the second is that with PCL diol

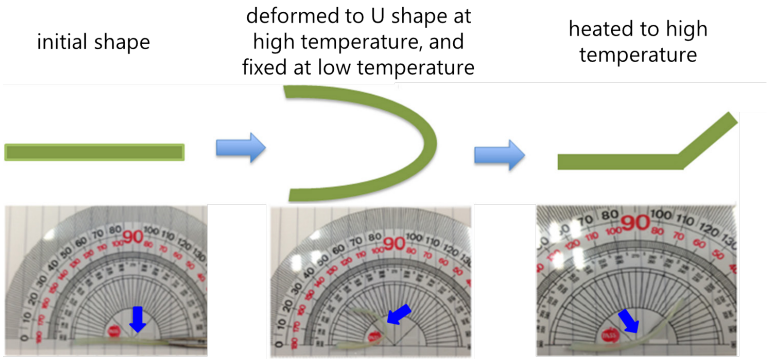

Fig. 2: Evaluation of the shape-memory process. [Reproduced from Ref. 1]

and poly-lactic-acid diol (PLLA diol) in ratio 8:2 in the soft domains, and the third is that with PCL diol and PLLA diol in ratio 6:4 in the soft domains. These three materials are abbreviated as PCL100, PCL80LL20 and PCL60LL40, respectively.

After synthesis of the three elastomers, experiments[1] were conducted to verify their shape memory. A standard memory test was performed with U-bending, as summarized in **Fig. 2**. Materials were cut to 4 cm × 0.05 cm and maintained at 50 °C for 5 min to make a U shape. This shape was retained at -18 °C for 10 min to implant the memory (fixation); we measured angle θ_A to calculate the shape fixation ratios. After the installation of the memory, we put the material at 50 °C for 5 min again to make it revert to the predesigned shape, and we measured angle θ_B to calculate the shape-recovery ratios.

$$\text{Shape fixationratio (\%)} = \frac{\theta_A}{180} \times 100\%$$

$$\text{Shape recovery ratio (\%)} = \frac{180 - \theta_B}{180} \times 100\%$$

The shape-fixation and recovery ratios for the three model polymeric elastomers are shown in **Table 1**. PCL100 showed small fixation but large recovery ratios; *i.e.* it exhibits the nature of a rubber, and was lacking memory. PCL80LL20 shows large fixation but small recovery ratios; *i.e.* it can be easily installed, but is difficult to revert. Finally, PCL60LL40 shows appropriate fixation and recovery ratios, characteristic of shape-memory materials. The results reveal that the various elastic soft domains give rise to varied shape-meqmory properties. Only the latter polymer has overcome the dilemma of fixation and recovery for an elastomer with both fixation and recovery ratios greater than 80%. In particular, this polymer demonstrated almost 100% recovery in water at 37 °C. Why? To reveal the secret of the shape-memory effect in polyurethane, we conducted small- and wide-angle X-ray scattering combined with a tensile tester *in situ.*

We conducted the tensile test first on PCL100, for which we observed a large maximum in the WAXS profile, which means that the structure of PCL diol is amorphous *i.e.* the entire molecular struc-

Table 1: Shape-fixation and recovery ratios of each material. The shape-memory test was performed with two cycles. [Reproduced from Ref. 1]

Polyurethane samples	Cycle 1		Cycle 2	
	Fixation (%)	Recovery (%)	Fixation (%)	Recovery (%)
PCL100	36 ± 3.4	100 ± 0	41.6 ± 7.1	88.8 ± 2.3
PCL80LL20	100 ± 0	38.8 ± 7.5	100 ± 0	28 ± 3.5
PCL60LL40	74.5 ± 5.0	87.2 ± 3.8	80.5 ± 5.2	85.9 ± 4.4 (~100% in water at 37 °C)

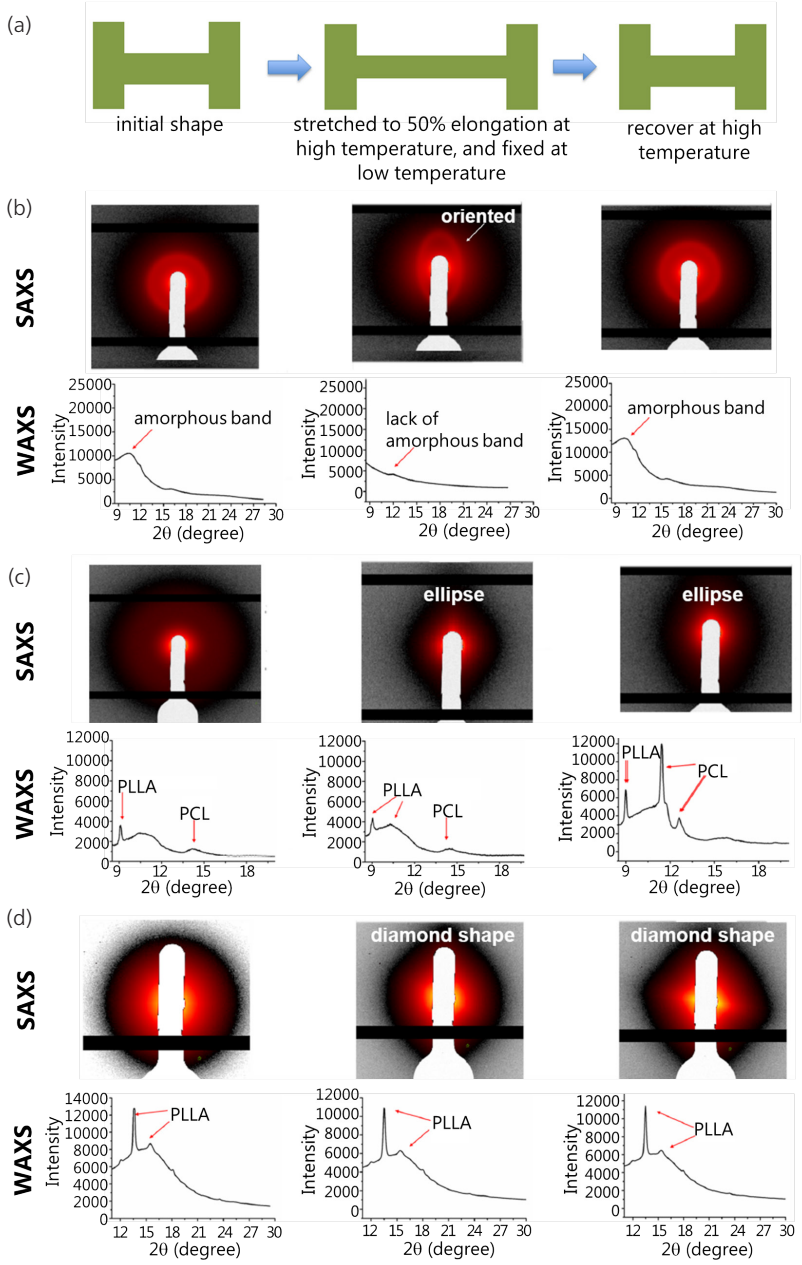

Fig. 3: (a) For WAXS/SAXS *in situ*, the film was installed on the tensile tester. Two-dimensional (2D) SAXS and WAXS patterns were recorded during the shape-memory test *in situ* for (b) PCL100, (c) PCL80LL20 and (d) PCL60LL40. [Reproduced from Ref. 1]

ture is like a big spring. As we released the spring, it recovered its shape immediately; for that reason PCL100 exhibited no significant shape fixation. PCL80LL20 exhibited sharp maxima in its WAXS profile; these maxima defined the crystallinity of PCL and PLLA, which can serve as bricks in the structure. The maxima of PCL shifted at the stretching stage. In contrast to the SAXS profile, the circular pattern transformed to elliptical from the initial stage; we thus believe that the random bricks are arranged in the same direction, which we call orientation at the stretching stage. At the recovery stage, the SAXS profile retained the elliptical pattern, which means that the oriented bricks did not revert to the initial state. PCL60LL40 showed PLLA crystallinity in its WAXS profile; this crystallinity exhibited no significant variation at each stage. The SAXS pattern demonstrated a diamond shape at the stretching stage and the recovery stage, which means that the bricks remained oriented during the stretching stage, but the PLLA oriented bricks did not interfere with the recovery of the material. Data curves of WAXS/SAXS are illustrated in **Fig. 3**. Based on these observations, we conclude that the installation of the shape is controlled with the brick structure, and the reversion effect is influenced by the spring structure. PCL and PLLA oriented crystallinity can both fix the shape, whereas the amorphous PCL chains assist the reversion effect. The PCL crystallinity induced amorphous PCL to acquire oriented PCL crystallinity (indicated by the diminished maximum in the WAXS profile), but the PLLA crystallinity did not influence the amorphous PCL. The spring structure can hence help recover the shape in the case of PCL60LL40.

Using the tensile tester *in situ* linked with the **TLS 23A1** SAXS facilities, a brand new mechanism for the reversion of biodegradable rubber was unveiled. First, the amorphous PCL chains constitute the element that is responsible for the reversion. Second, the oriented crystalline PLLA chains are the main element that is responsible

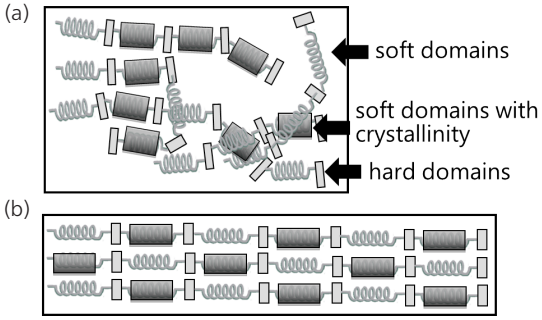

Fig. 4: (a) Schematics of polyurethane elastomer that consists of soft domains and hard domains. Soft domains might be chosen from biodegradable and crystalline polymeric materials (such as PLLA) for complete degradation to occur subsequently in a human body. (b) The crystalline soft domains (black blocks) serve as the fixing elements during the shape deformation processing. [Reproduced from Ref. 1]

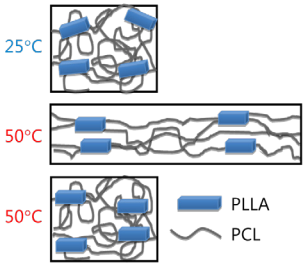

Fig. 5: The new mechanism revealed in this work for the shape-memory and recovery process under air at 50 °C (*i.e.* thermal switch = 50 °C). The amorphous PCL segments in polyurethane are responsible for recovery; the oriented PLLA segments act as the fixing element. [Reproduced from Ref. 1]

for the memorization; switching the memory is hence based on the orientation instead of the degree of crystallinity. Third, molecules of water provide an extra driving force for the reversion, instead of temperature (a thermal switch) alone. Fourth, the oriented PLLA chains do not interfere with the elasticity of the entire polyurethane molecule; *i.e.*, this rubber with an effective memory is still a rubber! Finally, all these soft chain elements are biodegradable, thanks to the modular structural versatility of polyurethane! Just plug in your design. The story of this new mechanism is portrayed in **Figs. 4 and 5**. The story is incomplete: the design of the biodegradable shape-memory elastomer (PCL60LL40) has practical applications. A sequel to this story, concerning the practical use in prospectively filling a bone defect and other biomedical applications, will be published in 2018. (Reported by Shan-hui Hsu, National Taiwan University)

This report features the work of Shan-Hui Hsu and her co-workers published in ACS Appl. Mater. Interfaces ***9****, 5419 (2017).*

TLS 23A IASW – Small/Wide Angle X-ray Scattering

- SAXS and WAXS *in situ*
- Soft Matter

Reference

1. Y. C. Chien, W. T. Chuang, U. S. Jeng, and S. H. Hsu ACS Appl. Mater. Interfaces, **9**, 5419 (2017).

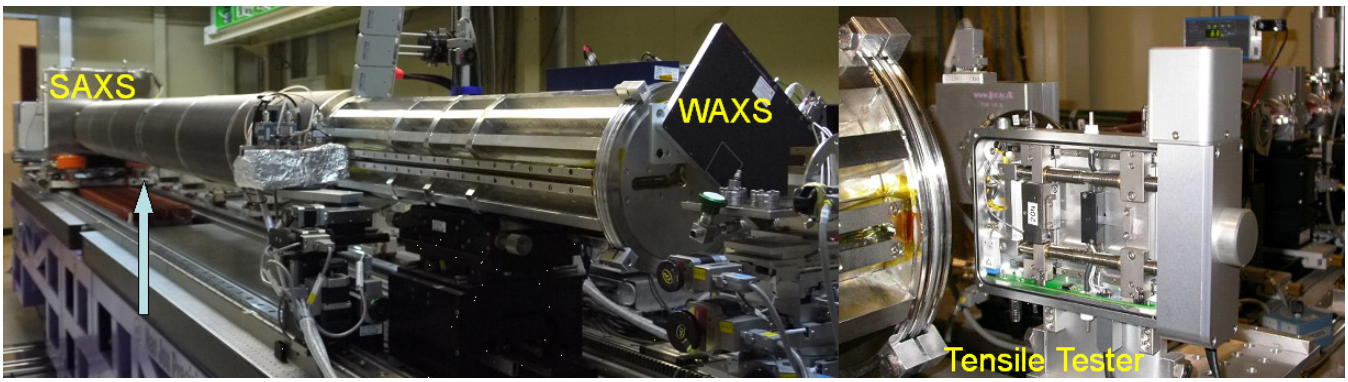

TLS 23A1 Small/Wide-angle X-ray Scattering